

Fluorescence Sensor Design for Transition Metal Ions: The Role of the PIET Interaction Efficiency

Ramachandram Badugu^{1,2}

Received May 12, 2004; accepted June 21, 2004

Multicomponent systems **1**, **2**, and **3** having *fluorophore-spacer-receptor* architecture have been prepared with a view to understand the role of the photoinduced intramolecular electron transfer (PIET) interactions in transition metal ion sensing efficiency of these systems. Structurally similar compounds 4-amino-1,8-naphthalimide (**4**), 4-aminophthalimide (**5**), and 4-methoxy-1,8-naphthalimide (**6**) were used as the *fluorophore* moieties. Dimethylamino group (as in the case of **1a**, **2a**, and **3a**, series A) and an aniline moiety (like in **1b**, **2b**, and **3b**, series B) have been employed as the *receptor* components. A two-carbon ethylene chain serves as a *spacer* unit. The absorption and fluorescence spectral features of the systems have been studied in the absence and presence of various transition metal ions. All the multicomponent systems (except **1a**) show weak fluorescence intensities compared to that of their constituent fluorophores (**4**, **5**, and **6**) in any given solvent. The reason for this low fluorescence quantum yield could be ascribed to the efficient PIET interaction between receptor moiety and the electron deficient fluorophore component of the systems. This has been corroborated with the estimated thermodynamic driving force (ΔG^*) for the PIET process in the multicomponent systems, calculated using electrochemical and spectral properties of individual components, is more negative for **2** and **3** than for **1** having electron deficient fluorophores **5**, and **6**, respectively. Especially, as evidenced by their low fluorescence quantum yield values, the PIET interaction is found to be more significant in the systems of series B (**1b**, **2b**, and **3b**) than the respective system of series A (**1a**, **2a**, and **3a**, respectively). The sensing capability of the systems is directly related to the efficiency of the PIET interaction in the unbound state. Accordingly, all these systems (except **1a**) show significant fluorescence enhancement in the presence of transition metal ions, well known for their high fluorescence quenching behavior. The present paper describes, the feasibility of optimizing the PIET interaction in the multicomponent sensor system in unbound state, and thus transition metal ion signaling capability of the system.

KEY WORDS: Fluorescence sensors; PIET interaction; transition metal ions; sensing.

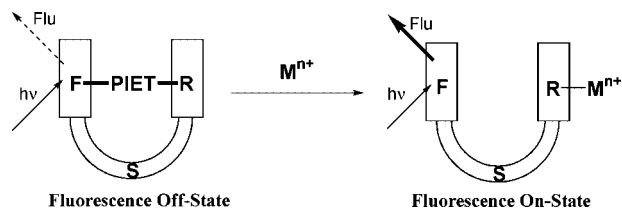
INTRODUCTION

The design and development of multicomponent systems capable of performing light induced logic operations such as sensing of a guest species is an interesting area of the current research [1,2]. Fluorosensors, which have been developed in the recent years, are known to be simple

and elegant in the detection of various analytes including cations, anions, neutral molecules, etc [2]. Most of the developed fluorosensors are supramolecular assemblies whose components perform one or more specific functions such as light absorption and emission (ca. *fluorophore*), an event of complexation and decomplexation of the guest species (ca. *receptor*). The two components, fluorophore and receptor, are often connected with a spacer unit, usually a saturated carbon chain with a varied chain length, giving rise to a *fluorophore-spacer-receptor* architecture for multicomponent sensor systems (Scheme 1) [2]. In the construction of fluorosensors, it is understood from the abundance of literature on this topic, the photoinduced

¹ School of Chemistry, University of Hyderabad, Hyderabad 500 046, India.

² To whom correspondence should be addressed at Center for Fluorescence Spectroscopy, University of Maryland School of Medicine, 725 West Lombard Street, Baltimore, Maryland 21201, USA. E-mail: badugu@cfs.umbi.umd.edu



Scheme 1. Fluorescence signaling mechanism.

intramolecular electron transfer (PIET) interaction between the fluorophore and receptor is the most commonly exploited mechanism. In the presence of guest species, guest induced modulations in the extent of PIET interaction governs the nature of the output signal of that system; it may lead to fluorescence enhancement [2] or quenching, [2e] depending on the sensor design. In the present case, we have chosen the sensor components (fluorophore and receptor) such that an efficient PIET interaction between them is operating in the absence of the metal ions, leading to fluorescence quenching of the system (Fluorescence Off-State). However, in the presence of the metal ions, as the result of the metal ion binding at the receptor site and thereby engaging the lone pair of electrons that are originally involved in the PIET process, the PIET communication between the components is turned-off. This leads to fluorescence recovery of the system (Fluorescence On-State). Thus, the presence of the metal ions in the medium is signaled by fluorescence “switching-on” of the sensor system. In other words, fluorescence enhancement (FE) is observed in the presence of the notorious quenching transition metal ions. The fluorescence signaling mechanism in the present systems is illustrated schematically in Scheme 1; where ‘F, S, and R’ are identify the fluorophore, spacer, and receptor moieties, respectively.

Amines or nitrogen rich molecules are generally used as the receptor components in the construction of fluorosensors for the detection of transition metal ions with a *fluorophore-spacer-receptor* architecture [3,4]. However, because of efficient fluorescence quenching nature of transition metal ions [5,6] very low or no FE has been observed for various systems [3] including **1a** (Chart 1), constructed using this format [7]. To circumvent the fluorescence quenching nature of transition metal ions, one can adopt two different approaches: (1) development of a receptor with a special recognition topology, which can also act as an insulator between the quenching transition metal ions and the fluorophore and (2) direct minimization of the interaction between the quenching metal ion and fluorophore. Ghosh *et al.* [4a], also very recently Banthia and Samanta [4b] have used the former strategy, in which the

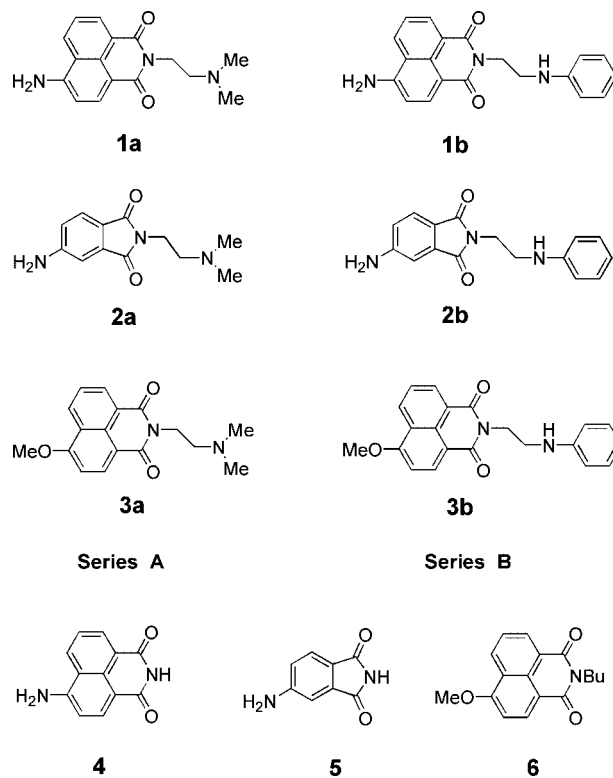


Chart 1. Sensor systems (**1**, **2**, and **3**) and fluorophores (**4**, **5**, and **6**).

encapsulation of transition metal ions into a cryptand cavity (receptor) minimizes the quenching influence of transition metal ions on the fluorophore and avoiding metal-fluorophore (quenching) interactions. Although, this is an elegant approach to overriding the quenching influence of the transition metal ions, it requires considerable synthetic effort. Also, systems developed with this approach are quite complex and difficult to implement in real-time applications. This approach may not be successful with every system developed as the metal sensing efficiency of a sensor system is solely dependent on the extent of PIET interaction in the unbound-state of that system rather than the efficiency of insulation of the quenching transition metal ions by a specially designed receptor component [4b]. When one need to construct an off-on fluorescence sensor system for transition metal ions, it is necessary to consider three issues: (a) fluorophore-metal ion interaction, which is largely redox in nature [5,6] and leads to the fluorescence quenching, (b) receptor-metal ion interaction that causes the FE because of reduced PIET interaction in the metal bound state, and (c) the efficiency of the PIET interaction between the components in the unbound state, which dictates the expected FE in the presence of a guest. Simultaneous achievement

of an efficient PIET communication and reduced metal–fluorophore interaction can be possible simply by choosing an “electron deficient fluorophore” in the construction of the multicomponent fluorescence sensor. Using this logical approach of “fluorophore selection/modulation,” we have developed several systems that show fairly good FE values in the presence of transition metal ions [7–13]. Systems **1** (especially **1a**), with electron rich 4-amino-1,8-naphthalimide (**4**) as the fluorophore moiety, are inefficient towards the detection of transition metal ions. This failure can be ascribed to the poor PIET interaction in these systems. On the basis of the present fluorophore design strategy, an improvement in the PIET communication can be expected in the multicomponent systems **2** and **3**, which consist of electron deficient fluorophores, 4-aminophthalimide (**5**) and 4-methoxy-1,8-naphthalimide (**6**), respectively. The same was supported by their low quantum yields in the absence of transition metal ions. Also as it is stated in the introduction, numerous investigations have been made on the topic of fluorescence sensing using PIET mechanism for the detection of various analytes. However, the significance of the extent of the PIET communication in the sensing event is rarely addressed. In this article, we have made an attempt to understand the role of the PIET interaction efficiency towards the metal ion sensing capability of three sets of sensor systems shown in Chart 1.

EXPERIMENTAL SECTION

Materials

Compounds, 4-amino-1,8-naphthalic anhydride, *N,N*-dimethylethylenediamine and *N*-phenylethylenediamine (Aldrich) and 4-chloro-1,8-naphthalic anhydride (Acros Organics) were used without further purification for the synthesis of multicomponent systems. The fluorophores, 4-aminophthalimide (Kodak) and 4-amino-1,8-naphthalimide (Aldrich), used in the spectral measurements were recrystallized several times from aqueous ethanol. Acetonitrile (AN), *N,N*-dimethylformamide (DMF) and tetrahydrofuran (THF) were purchased from Merck (India). Analytical grade metal salts, $\text{Zn}(\text{H}_2\text{O})_6(\text{ClO}_4)_2$, $\text{Cu}(\text{H}_2\text{O})_3(\text{NO}_3)_2$, $\text{Ni}(\text{H}_2\text{O})_6(\text{ClO}_4)_2$, $\text{Co}(\text{H}_2\text{O})_6(\text{NO}_3)_2$, $\text{Fe}(\text{H}_2\text{O})_6(\text{ClO}_4)_2$, $\text{Mn}(\text{H}_2\text{O})_6(\text{ClO}_4)_2$, and $\text{Cr}(\text{H}_2\text{O})_6\text{Cl}_2$ (Loba, India), used as received. The solvents, THF and AN used in the spectral studies have been rigorously purified by standard procedures [14], and transparent in the spectral region of interest. Further, it was confirmed by the measurement of $E_T(30)$ values [15] that the solvents (THF and AN) employed in the spectral study are free from moisture and polar impurities.

Preparation of the Systems

For the synthesis of **1a** and **1b**, a common procedure was used as described below for **1a**. For the preparation of **1b**, *N*-phenylethylenediamine is used instead of *N,N*-dimethylethylenediamine. Fluorosensor **1a** was obtained by refluxing an ethanolic suspension of 4-amino-1,8-naphthalic anhydride (0.10 g, 0.47 mmol) with *N,N*-dimethylethylenediamine (0.06 mL, 0.56 mmol) for 24 hr. After complete reaction, the solvent was evaporated under reduced pressure and the residue obtained was purified using column chromatography.

Systems **2a** and **2b** were prepared using a general procedure outlined below for **2a**. Sensor **2b** was obtained when *N*-phenylethylenediamine is used instead of *N,N*-dimethylethylenediamine. In a 10 mL round bottomed flask fitted with a water condenser and potassium hydroxide guard tube, 4-aminophthalimide (0.50 g, 3.08 mmol) and *N,N*-dimethylethylenediamine (0.40 mL, 3.69 mmol) were combined, and the mixture was heated at 80°C with constant stirring for about 5 hr. The viscous product thus obtained was purified by column chromatography.

Fluorosensors **3a**, **3b** and constituent fluorophore **6** were prepared using a two-step method. In the first step, an ethanolic suspension of 4-chloro-1,8-naphthalic anhydride (0.50 g, 2.15 mmol) in 5 mL ethanol was refluxed with an equimolar amount of an appropriate amine (*N,N*-dimethylethylenediamine for **3a**, *N*-phenylethylenediamine for **3b** and *n*-butylamine for **6**) for 6 hr. Then the reaction mixtures were allowed to cool to room temperature. The solid products crystallized out upon cooling, and were filtered using a funnel and dried under vacuum. In the second step, a portion of the solid product, obtained in the previous step, was dissolved in DMF (5 mL) and treated with sodium methoxide (0.10 M methanol solution, 5 mL) at room temperature for 6 hr. The solvent was removed under vacuum and the residue was purified using column chromatography.³

³ Spectral data of fluorosensors **1–3** and fluorophore **6**. System **1a**: Yield 75%. IR (KBr, cm^{-1}): 3402, 3211, 2943, 2813, 1672, 1639, 1375, 771, and 754; ¹H NMR (CDCl_3): δ 2.5 (s, 6H), 2.7 (t, 2H), 4.2 (t, 2H), 5.1 (s, 2H), 6.8 (d, 1H), 7.6 (t, 1H), 8.0 (d, 1H), 8.3 (d, 1H), and 8.6 (d, 1H). **1b**: Yield 70%. IR (KBr, cm^{-1}): 3468, 3350, 3234, 3040, 2831, 1670, 1639, 1365, 769, and 752; ¹H NMR (CDCl_3): δ 3.6 (t, 2H), 4.2 (s, 1H), 4.5 (t, 2H), 5.0 (s, 2H), 6.6 (m, 3H), 6.9 (d, 1H), 7.1 (t, 2H), 7.7 (t, 1H), 8.1 (d, 1H), 8.4 (d, 1H), and 8.6 (d, 1H). **2a**: Yield 80%. IR (KBr, cm^{-1}): 3429, 3350, 2926, 2852, 1759, 1697, 1396, 1010, and 748; ¹H NMR (MeOH-d_4): δ 2.6 (s, 6H), 3.0 (t, 2H), 3.6 (t, 2H), 5.2 (s, 2H), 6.9 (dd, 1H), 7.2 (d, 1H), and 7.6 (d, 1H). **2b**: Yield 75%. IR (KBr, cm^{-1}): 3477, 3373, 3250, 3040, 2922, 1759, 1687, 1008, and 745; ¹H NMR (CDCl_3): δ 3.4 (t, 2H), 3.9 (t, 2H), 4.4 (s, 1H), 5.2 (s, 2H) 6.6 (m, 3H), 6.8 (dd, 1H), 7.0 (d, 1H), 7.2 (t, 2H), and 7.6 (d, 1H). **3a**: Yield 70%. IR (KBr, cm^{-1}): 2943, 1697, 1657, 1593, 1388, 1028, and 779.

Methods and Apparatus

Room temperature NMR spectra of the compounds were recorded on Bruker ACF-200 spectrometer. Infrared spectra were recorded on a JASCO FT-IR/5300 spectrometer. The absorption and fluorescence spectra were recorded on a JASCO UV-Vis spectrophotometer (model 7800) and JASCO spectrofluorometer (model FP-777), respectively. The fluorescence decay curves were measured using a single photon counting spectrofluorometer (IBH-5000). The instrument was operated using a thyatron-gated flash lamp filled with hydrogen at a pressure of 0.5 atmospheres, and the distance between the electrodes was maintained at 1 mm. The lamp, having the pulse width of ~ 1.2 ns, was operated at a frequency of 40 kHz. The lifetimes were estimated from the measured fluorescence decay curves and the lamp profiles using a nonlinear least-squares iterative fitting procedure [16]. The quality of the fit was assessed by the plot of the standard deviation and the chi-square values. The cyclic voltammetric measurements were carried out on Cypress model CS-1090/CS-1087 computer controlled electroanalytical system. Ag/AgCl was used as reference electrode, a glassy carbon as the working electrode and a platinum wire as the auxiliary electrode. The redox potentials were measured in nitrogen bubbled acetonitrile using 0.1 M tetrabutylammonium perchlorate as the supporting electrolyte. The scanning speed was maintained at 100 mV/s.

The fluorescence quantum yields of **1** were measured using coumarin C-153 ($\phi_f = 0.89$ in acetonitrile) [17] as a reference compound, and those of **2** and **3** were obtained by comparison with that of fluorophore **5** in acetonitrile ($\phi_f = 0.63$) [18]. A solution of **1**, **2** and **3** in acetonitrile or in THF was prepared with the same absorbance ($A \sim 0.2$) as that of the reference compounds in acetonitrile at the exciting wavelengths ($\lambda_{ex} = 425$ nm for **1**, 400 nm for **2**, and 350 nm for **3** and **6**). The fluorescence spectra of the reference and sample compounds were measured under the same experimental conditions

¹H NMR (CDCl₃): δ 2.3 (s, 6H), 2.6 (t, 2H), 4.1 (s, 3H), 4.4 (t, 2H), 7.0 (d, 1H), 7.6 (t, 1H), and 8.5 (m, 3H). **3b**: Yield 60%. IR (KBr, cm⁻¹): 3275, 3030, 2960, 1697, 1651, 1388, 1263, 1053, and 781. ¹H NMR (CDCl₃): δ 3.5 (t, 2H), 4.1 (s, 3H), 4.3 (s, 1H), 4.6 (t, 2H), 6.6 (dd, 3H), 6.9 (d, 1H), 7.1 (t, 2H), 7.5 (t, 1H), and 8.5 (m, 3H). **6**: Yield 70%. IR (KBr, cm⁻¹): 2957, 2850, 1693, 1657, 1593, 1026, and 781; ¹H NMR (CDCl₃): δ 0.9 (t, 3H), 1.5 (m, 2H), 1.7 (m, 2H), 4.1 (s, 3H), 4.2 (t, 2H), 6.9 (d, 1H), 7.6 (t, 1H), and 8.4 (m, 3H). The presented data is consistent with the data reported for the similar systems in literature. See for example, V. Wintgens, P. Valat, J. Kossanyi, A. Demeter, L. Biczók, and T. Bérces (1996). Spectroscopic properties of aromatic dicarboximides. 4. On the modification of the fluorescence and intersystem crossing processes of molecules by electron-donating methoxy groups at different positions. The case of 1,8-naphthalimides, *New J. Chem.*, **20** (11), 1149–1158 and references cited therein.

and settings. The quantum yields were obtained from measurements of the areas underneath the fluorescence spectra. The fluorescence measurements were carried out using $\sim 10^{-5}$ M solutions of the fluorosensors. The effect of the metal ions on the fluorescence intensity was examined by adding a few μ L of a stock solution of the corresponding metal salts in the same solvent to a known volume (2 mL) of solutions of **1**, **2**, and **3**. The addition was limited to 100 μ L to minimize the volume change.

RESULTS

Electrochemical Data

The redox potentials of the parent fluorophores **4**, **5**, and **6** have been examined to explore the electronic nature of the fluorophores. While oxidation potentials were observed at 1.27, and 1.50 V [7] for **4** and **5**, respectively, no corresponding peak could be observed for **6** in the range of 0–2 V. This observation clearly indicates that **5** and **6** are more electron deficient than **4**. Hence, according to the present design logic, the multicomponent systems **2** and **3** are expected to be superior over **1** as fluorescence off-on sensor systems for transition metal ions. The observed reduction potentials for **4**, **5**, and **6** (–1.61, –1.66, and –1.11 V, respectively) are consistent with the structures of these compounds [19]⁴.

Photophysical Properties

The absorption and fluorescence spectra of **1**, **2**, and **3** are found to be similar to those of their respective parent fluorophores in any given solvent (Fig. 1). The broad, structure less and solvent sensitive behavior of fluorescence spectra of **2** and **3** indicate the occurrence of an intramolecular charge transfer (ICT) from 4-amino nitrogen to imido-oxygens in a process similar to that observed in the parent fluorophores **4** and **5** [18,20]. Absorption and fluorescence spectra of **6** in two solvents, hexane and acetonitrile, are shown in Fig. 2. Fluorophore **6** and sensor systems **3** show structured absorption and fluorescence bands in nonpolar solvents such as hexane, which could be ascribed to the lowest π, π^* transitions [12,21]. On the other hand, in polar solvents, a considerable solvent polarity induced red shift in the band maximum is noticed

⁴ Compounds **4** and **6** with electron-donating groups at 4-position are difficult to get reduce than the parent system 1,8-naphthalimide: the observed reduction potentials of **4**, **6**, and 1,8-naphthalimide are –1.61, –1.11, and –1.00 V, respectively. A similar kind of explanation has been ascribed in the literature to explain the substituent effect on the redox behavior of various compounds, see ref. [19].

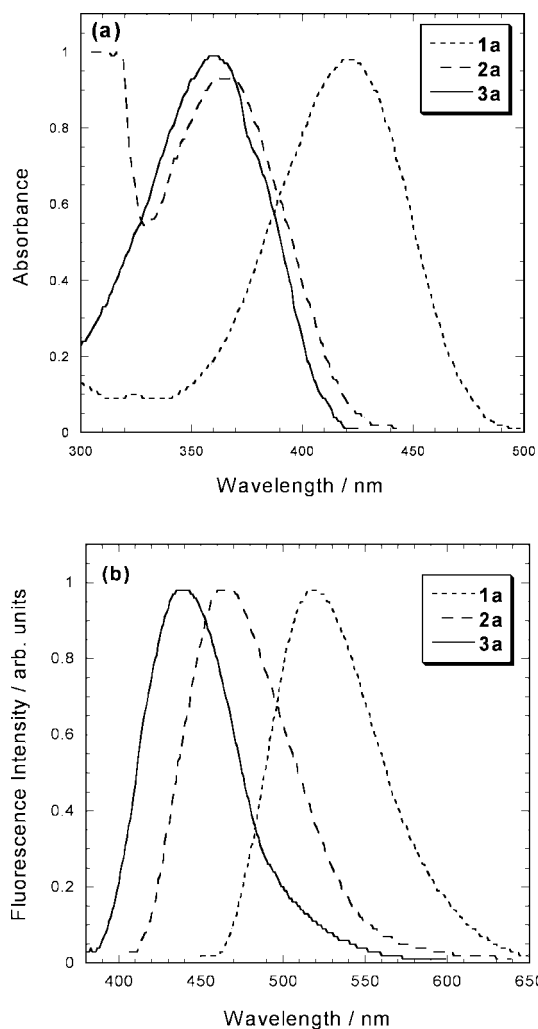


Fig. 1. Absorption (a) and fluorescence (b) spectra of **1a**, **2a**, and **3a** ($\sim 10^{-5}$ M) in acetonitrile. The excitation wavelengths were 425, 400, and 350 nm for **1a**, **2a**, and **3a**, respectively. The fluorescence intensities of the systems have been normalized at the band maximum for clarity.

(Table I). Also band broadening (full-width at half maximum, FWHM, in hexane and acetonitrile are 3815 cm^{-1} and 4325 cm^{-1} , respectively) especially in the longer wavelength region of the absorption spectrum was observed in polar solvents. Moreover, more significant solvent polarity induced spectral changes were noticed in the fluorescence spectrum (see Fig. 2). This can be understood assuming the close proximity of the two excited states, π, π^* and the ICT in these systems [22]. The fluorescence excitation spectra, recorded to establish the nature of the emitting states, with structured and comparable band position to that of the absorption band in hexane and structure less, red shifted ($\sim 8\text{ nm}$) with respect to the absorption band maximum in acetonitrile, confirm the close proxim-

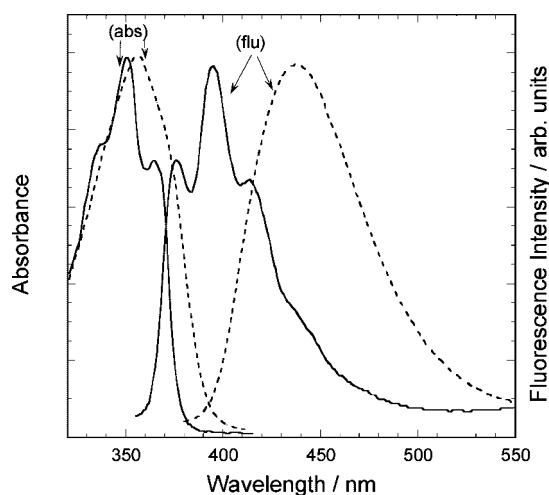


Fig. 2. Absorption and fluorescence spectra of **6** in hexane (—) and in acetonitrile (- - -). $\lambda_{\text{ex}} = 350\text{ nm}$. The fluorescence intensities were normalized at band maximum for clarity.

ity of the two excited states. The ICT state is lowest in energy from which a structure less fluorescence has been observed in polar solvents such as THF and AN [22]. The fluorescence from an ICT excited state is made possible for two reasons: (1) the enhanced electron donating nature of the methoxy group in the excited state and (2) significant solvent stabilization of the excited ICT state over the solvent insensitive π, π^* state. The absorption and fluorescence band maxima of **1** is red shifted when compare to those of **2** and **3** in any given solvent (Table I). This behavior (especially when **1** and **3** are considered) can be understood by taking into consideration of the difference in the electron-donating ability of the substituent at the 4-position of the fluorophore. The spectral data of **1**, **2**, and **3** along with those for constituent fluorophores for comparison in THF and AN have been collected in Table I. All the compounds exhibit solvatochromism, as is expected for a charge transfer band and the extent of red shift in the band location is more significant in the fluorescence spectrum, indicating a more polar excited state than ground state [18,20,23].

The fluorescence quantum yields of the multicomponent systems and the constituent fluorophores are shown in Table II. Fluorophores, 4-Amino-1,8-naphthalimide (**4**) [22,24] and 4-aminophthalimide (**5**) are usually highly fluorescent in nonhydrogen bonding solvents [18,25]. As is shown in the table, fluorophore **6** also exhibits quite high fluorescence intensities in the two solvents, THF and acetonitrile. On the other hand, the multicomponent systems **1**, **2**, and **3** show considerable reduction in their fluorescence quantum yields with respect to the constituent fluorophores in any given solvent. Also, the fluorescence

Table I. Absorption and Fluorescence Spectral Data of Multicomponent Systems and Constituent Fluorophores in THF and AN^a

Compound	Tetrahydrofuran		Acetonitrile	
	$\lambda_{\max}(\text{abs})$ (nm)	$\lambda_{\max}(\text{flu})^b$ (nm)	$\lambda_{\max}(\text{abs})$ (nm)	$\lambda_{\max}(\text{flu})^b$ (nm)
1a	415	510	422	520
1b	417	512	421	520
4	412	498	420	510
2a	361	461	365	466
2b	366	463	366	468
5	358	455	359	460
3a	340 (sh), 359, 375 (sh) ^c	436	345 (sh), 360, 375 (sh)	439
3b	340 (sh), 360, 375 (sh)	428	340 (sh), 362, 375 (sh)	437
6	345 (sh), 354, 375 (sh)	427	340 (sh), 357, 375 (sh)	438

^a ±2 nm.^b Fluorescence spectra were measured on excitation at 425 nm for **1** and **4**, 400 nm for **2** and **5**, and 350 nm for **3** and **6**.^c (sh) Represents a shoulder.

quantum yields of **1**, **2**, and **3** are decreased with increasing solvent polarity (from THF to AN). The trend in the quantum yields with solvent polarity is very similar with that of similar *donor-spacer-acceptor* systems in the literature [26]. However, sensor **3b** shows relatively higher fluorescence quantum yield in AN than in THF. This may be explained by considering the electron-donating and accepting abilities of donor and acceptor moieties, respectively, and orientations and effective distance between the reacting components (fluorophore and receptor) in various solvents. In other words the quantum yields are related to the apparent rate constants for the electron transfer process in these systems in various solvents [27,28] and the

electron transfer mechanism. It is evident from Table II that comparatively lower fluorescence quantum yields are observed for the systems of series B, containing aniline moiety as the receptor (**1b**, **2b**, and **3b**) than for the respective systems of series A (**1a**, **2a**, and **3a**). The factor (f)⁵ of reduction in the fluorescence quantum yield of a multicomponent system with respect to the corresponding fluorophore is also shown in Table II.

The fluorescence decay behavior of these systems was studied using a nanosecond time-resolved instrument. A few representative fluorescence decay curves measured for fluorophore **4** and multicomponent system **1b** in acetonitrile are depicted in Fig. 3. As can be seen from the figure, fluorophore **4** displays a single exponential decay in any given solvent. The same is true for the other fluorophores, **5** and **6**. On the other hand, the decay behavior for any multicomponent system is clearly biexponential and thus can be best fitted to the function, $I(t) = \alpha_1 \exp(-t/\tau_1) + \alpha_2 \exp(-t/\tau_2)$ in both solvents, THF and AN. The fluorescence decay parameters for all the compounds in THF and AN are depicted in Table III. The percentage of the short-lived components, in which the PIET interaction is more efficient, is more for the systems having electron deficient fluorophores. A further increase in the percentages of short-lived components has been observed for systems of series B as compared to those of series A with the same fluorophore.

Table II. Fluorescence Quantum Yields^a of **1**, **2**, and **3** and Constituent Fluorophores, **4**, **5**, and **6**, in Tetrahydrofuran and Acetonitrile^b

Compound	Tetrahydrofuran	f^b	Acetonitrile	f^b
1a	0.67	1.5	0.74	1.3
2a	2.3×10^{-2}	30	1.3×10^{-2}	50
3a	6.5×10^{-2}	12	3.9×10^{-2}	20
1b	2.9×10^{-2}	34.5	3.0×10^{-2}	32
2b	5.8×10^{-4}	2000	2.6×10^{-4}	2450
3b	2.3×10^{-4}	3225	1.15×10^{-3}	680
4	1.0	–	0.97	–
5	0.70 ^c	–	0.63 ^c	–
6	0.76	–	0.78	–

^a ±5% for values of 10^{-2} or higher and ±10% for values less than 10^{-2} .^b Also shown is the factor (f) representing the ratio between the fluorescence quantum yields of the constituent fluorophore and the sensor system, which is equal to both expected FE in the presence of metal ions and the extent of PIET interaction between the fluorophore and receptor in the absence of the metal ions.^c From Ref. [18].⁵ The factor, f , is the experimental measure for the extent of PIET communication in the systems and one can expect the FE values equal to this in magnitude when PIET in the systems is completely cut-off in the presence of a non-quenching metal ion.

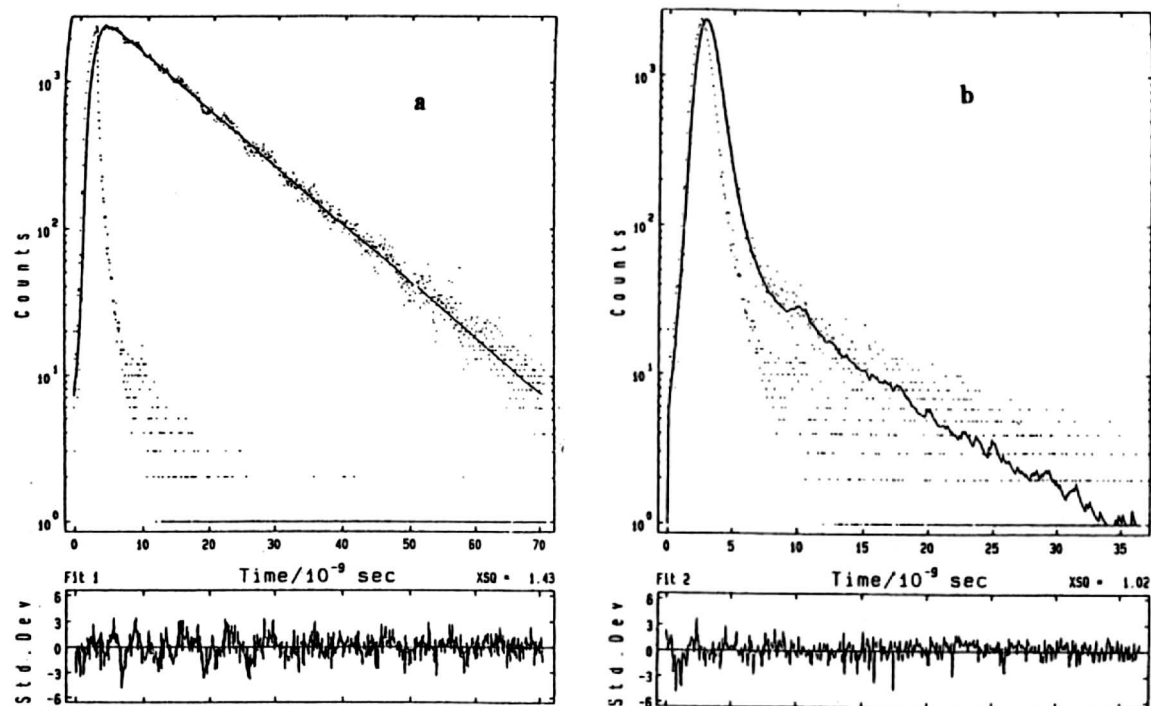


Fig. 3. Fluorescence decay profiles of (a) **4** and (b) **1b** in acetonitrile. The excitation wavelength was 425 nm. The fluorescence was monitored at the emission band maximum. Solid lines indicate the best fit to the measured decay profiles. The decay curve for multicomponent system **1b** was found to be best represented by a biexponential decay function while that of fluorophore **4** was found to be a single exponential. The excitation lamp profiles are also shown in the figure.

Table III. Fluorescence Lifetime (τ) Data of **1**, **2**, and **3** and Corresponding Parent Fluorophores (**4**, **5**, and **6**), Along with the Relative Amplitudes of the Lifetime Components in Tetrahydrofuran and Acetonitrile^{a,b}

Probe	Tetrahydrofuran				Acetonitrile			
	τ_1 (ns)	α_1	τ_2 (ns)	α_2	τ_1 (ns)	α_1	τ_2 (ns)	α_2
1a	0.8	7.0	6.9	93.0	2.2	2.0	7.4	98.0
2a	0.7	48.0	13	52.0	0.5	98.0	15.5	2.0
3a	0.4	74.0	7.2	6.0	0.1	97.0	8.2	3.0
1b	0.8	99.9	7.4	0.1	0.4	99.9	7.5	0.1
2b	0.9	95.0	12.2	5.0	0.2	99.0	12.1	1.0
3b	1.1	46.0	7.2	54.0	0.4	89.0	8.2	11.0
4	11.0	100	–	–	11.0	100	–	–
5	14.0	100	–	–	12.4	100	–	–
6	7.1	100	–	–	8.1	100	–	–

^aExcitation wavelengths were 425 nm for **1** and **4**, 400 nm for **2** and **5**, and 350 nm for **3** and **6**. Fluorescence decays were monitored at their emission band maxima.

^bAs the pulse width of the lamp used for the lifetime measurements is about 1.2 ns, error percentage of the lifetimes would be in the order of <5% for long-lived lifetime components and $\pm 5\%$ for short-lived lifetimes.

Effect of Metal Ions

After exploring the electrochemical and spectral properties of the sensor systems and fluorophores, we have studied transition metal ion induced spectral changes of all three sets of probes in two solvents, THF and AN, in the presence of transition metal ions.⁶ Since the metal ion binding to receptor is a ground state phenomenon, one may expect changes in the absorption spectra of these systems on addition of the metal ions. The absorption spectral changes are found to be different for different metal ions, and no general pattern could be observed for any system.⁷

⁶The effect of counter anion of the added transition metal salt on the fluorescence signaling of these probes is noticed to be minimum, and has been addressed briefly in earlier publications by the authors, see refs. [11 and 12].

⁷As the present receptor (dimethylamine and aniline) moieties are simple in their structure, estimation of the binding constants of the metal complexes, formed upon the addition of the metal salts, is impractical, and unimportant considering the following assumptions. It is genuine fact that one can assume the binding constants of a given metal ion with a specific receptor could be same, no matter what is the fluorophore component is. For example, the binding constants of Zn^{2+} with **1a**, **2a**, and **3a** should be similar in magnitude as the reacting components

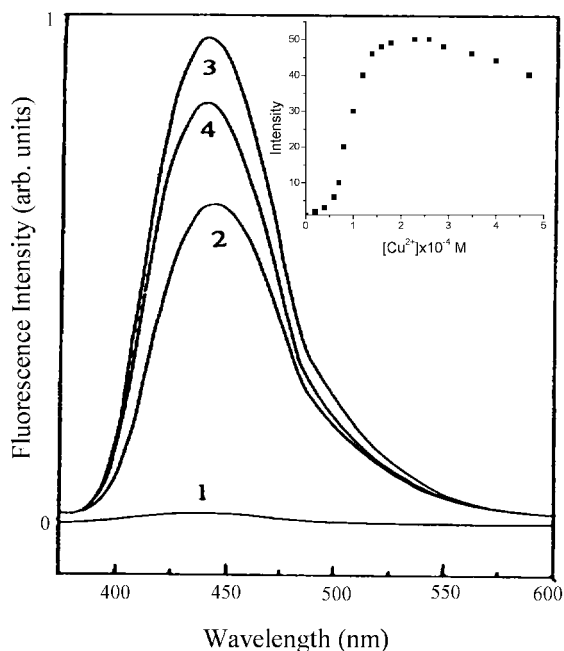


Fig. 4. Fluorescence emission spectra of **3b** ($\sim 10^{-5}$ M) in acetonitrile in the presence of various concentrations of $\text{Cu}(\text{H}_2\text{O})_3(\text{NO}_3)_2$. Cu^{2+} concentrations are (1) 0, (2) 1.2×10^{-4} , (3) 2.3×10^{-4} , and (4) 4.7×10^{-4} M. The excitation wavelength was 350 nm. Insert shows the response of the system with metal ion concentration.

This behavior is consistent with the varied coordination chemistry of the metal ions and may depend on the stability of the complexes [29]. However, in some cases a small red shift is noticed in the absorption spectrum in the presence of the metal ions. This could be due to the metal induced electronic redistribution in the system. The similar guest induced red shift in the absorption spectra of several systems having ICT fluorophore has been reported in the literature [2c,30,31].

Figure 4 shows the typical changes in the fluorescence spectrum of **3b** in acetonitrile in the presence of various amounts of $\text{Cu}(\text{H}_2\text{O})_3(\text{NO}_3)_2$. Fluorescence quenching by transition metal ions is a common phenomenon [5,6]. However, as can be seen from figure, the initial addition of the transition metal salts to the solutions of multicomponent systems leads to an increase in the fluorescence intensity of the systems and at a certain concentration the fluorescence intensity remains constant. Any further increase in the concentration of the metal ions causes the expected fluorescence quenching. The insert in Fig. 4 shows the fluorescence response of the system

(metal ion and receptor) are same. Hence an estimation of the binding constants is not important in this situation.

with the added metal ion concentration.⁷ The FE in the presence of the quenching transition metal ions could be explained using the scheme 1. As it is mentioned in introduction transition metal ions presence in the medium suppress the PIET interaction in the systems leading to the net FE. The observed FE values for **1**, **2**, and **3** in the presence of various transition metal ions in THF and AN are depicted in Tables IV and V. As can be seen, the observed FE values are extraordinarily high in some cases and the highest FE value could be observed for **3b** in the presences of Zn^{2+} , known as an inefficient quencher (Table V) [5,6]. It is worth noting that even in the presence of other notable quenching transition metal ions such as Fe^{3+} and Cr^{3+} , excellent FE values have been registered. The FE data presented in Tables IV and V indicates a direct relationship between the PIET efficiency of the systems and FE values, and inverse relation to the quenching efficiency of the metal ions. However, a fluorescence sensor system with an efficient PIET interaction can suitably show FE irrespective of the metal ion quenching efficiency as described in detail in fourth coming paragraphs.

Apart from FE, addition of the metal salts leads to increase in Stokes-shift of the systems. Since the locations of the emission band maxima of **4**, **5**, and **6** are sensitive to the polarity of the medium (Table I), the observed shift can in principle be due to the salt-induced increase in the polarity of the medium. However, since, the addition of the metal salts to the solutions of any parent fluorophore does not lead to any shift in its fluorescence band maximum, one can rule out the possibility that the spectral shift is due to salt induced change in the microscopic polarity around the fluorophore moiety. The shift might be due to the receptor assisted metal induced redistribution of the electronic charge in a donor acceptor system as mentioned for the ground state (metal induced absorption spectral change). A guest-induced red shift in the fluorescence spectrum has also been reported in the literature for sensor systems having an ICT fluorophore [2c,30,31].

The metal ion induced changes in the fluorescence decay behavior of the systems have also been studied. The typical changes in the fluorescence decay behavior of the systems on addition of the metal ions are depicted in Fig. 5. With the addition of the metal ions, the fluorescence decay profile of a multicomponent system changes from biexponential to a single exponential for concentrations of the metal ions corresponding to the maximum FE values. Further increase in the metal ion concentration leads to fluorescence quenching, as expected.

Table IV. Fluorescence Response of **1a**, **2a**, and **3a** as a Function of Different Metal Ions in Tetrahydrofuran and Acetonitrile^a

Metal Ion	1a				2a				3a			
	THF		AN		THF		AN		THF		AN	
	[M] ^b (mM)	FE ^{c,d}	[M] (mM)	FE	[M] (mM)	FE	[M] (mM)	FE	[M] (mM)	FE	[M] (mM)	FE
Cr ³⁺	0.290	1.4	0.043	1.1	0.810	38	0.120	39	0.460	8.0	0.500	26
Mn ²⁺	0.078	1.3	0.085	1.5	0.390	32	0.170	32	0.180	12	0.600	21
Fe ²⁺	0.042	1.3	0.026	1.1	0.100	33	0.100	34	0.065	12	0.370	15
Co ²⁺	0.130	1.4	0.011	1.1	3.100	12	0.190	38	0.800	10	0.470	26
Ni ²⁺	0.280	1.2	0.017	1.1	2.200	15	0.300	37	0.220	12	0.710	27
Cu ²⁺	0.900	1.3	0.025	1.2	3.700	19	0.270	41	0.350	9.0	0.350	23
Zn ²⁺	0.025	1.3	0.220	1.3	0.500	18	0.390	55	0.340	13	0.330	28

^aExperimental conditions: $\sim 2.0 \times 10^{-5}$ M solution of the compounds in tetrahydrofuran or acetonitrile was used at 298 K, $\lambda_{\text{ex}} = 425$ nm for **1a**, 400 nm for **2a**, and 350nm for **3a**, excitation and emission bandwidths were 3 nm.

^bRepresents the concentration of the metal ion for which the maximum FE was observed. Any further increase in the concentration led to fluorescence quenching.

^cWith reference to the fluorescence intensity of the respective compounds in the absence of the metal ions.

^d $\pm 5\%$.

DISCUSSION

While the oxidation potentials measured for the constituent fluorophores indicate the electron deficient nature of **5** and **6** over **4**, the measured reduction potentials and the spectral data allow us to estimate the thermodynamic feasibility for the PIET process in multicomponent systems (**1**, **2**, and **3**), in terms of the free energy change (ΔG^*). An estimation of ΔG^* values have been performed using the Weller equation, $\Delta G^* = E_{\text{ox}}(\text{receptor}) - E_{\text{red}}(\text{fluorophore}) - E_{0,0}$, where $E_{\text{ox}}(\text{receptor})$ represents the oxidation potential of the receptor moiety, $E_{\text{red}}(\text{fluorophore})$ denotes

the reduction potential of the fluorophore, and $E_{0,0}$ is the energy of the fluorescent state [32]. The $E_{0,0}$ values were estimated from the mean position of the absorption and fluorescence band maxima of fluorophores in acetonitrile. The oxidation potentials of triethylamine and *N*-methylaniline (0.49 and 0.50 V, respectively) are taken from reference [33]. The estimated ΔG^* values for various systems are presented in Table VI. Although, it is pertinent to note here that the PIET interaction is significantly less in systems **1** with electron rich **4** as the constituent fluorophore than that in **2** and **3**, the thermodynamic driving force for the PIET process is quite feasible for all three sets of compounds. Even though, the driving

Table V. Fluorescence Enhancement Data of **1b**, **2b**, and **3b** in the Presence of Various Metal Ions in Tetrahydrofuran and Acetonitrile^a

Metal Ion	1b				2b				3b			
	THF		AN		THF		AN		THF		AN	
	[M] ^b (mM)	FE ^{c,d}	[M] (mM)	FE	[M] (mM)	FE	[M] (mM)	FE	[M] (mM)	FE	[M] (mM)	FE
Cr ³⁺	2.90	4.0	3.00	8.0	100	130	3.80	210	100	1450	4.30	110
Mn ²⁺	3.50	17	0.60	14	9.70	300	4.70	680	2.40	2660	2.00	60
Fe ²⁺	0.17	5.0	0.22	21	1.70	15	5.10	350	0.13	2000	0.39	400
Co ²⁺	7.90	6.0	0.31	15	8.00	103	6.10	460	5.40	112	4.70	6.0
Ni ²⁺	0.48	23	1.00	5.0	2.80	10	0.77	500	2.30	19.0	2.00	5.5
Cu ²⁺	1.50	1.1	0.88	7.0	0.41	1.0	0.58	230	1.30	10.0	0.23	50
Zn ²⁺	2.90	1.1	5.70	2.0	0.14	85	0.12	800	0.11	2420	0.55	500

^aExperimental conditions: $\sim 2.0 \times 10^{-5}$ M solution of the compounds in tetrahydrofuran or acetonitrile was used at 298 K, $\lambda_{\text{ex}} = 425$ nm for **1b**, 400 nm for **2b**, and 350nm for **3b**, excitation and emission bandwidths were 3 nm.

^bRepresents the concentration of the metal ion for which the maximum FE was observed. Any further increase in the concentration led to fluorescence quenching.

^cWith reference to the fluorescence intensity of the respective compounds in the absence of the metal ions.

^d $\pm 5\%$.

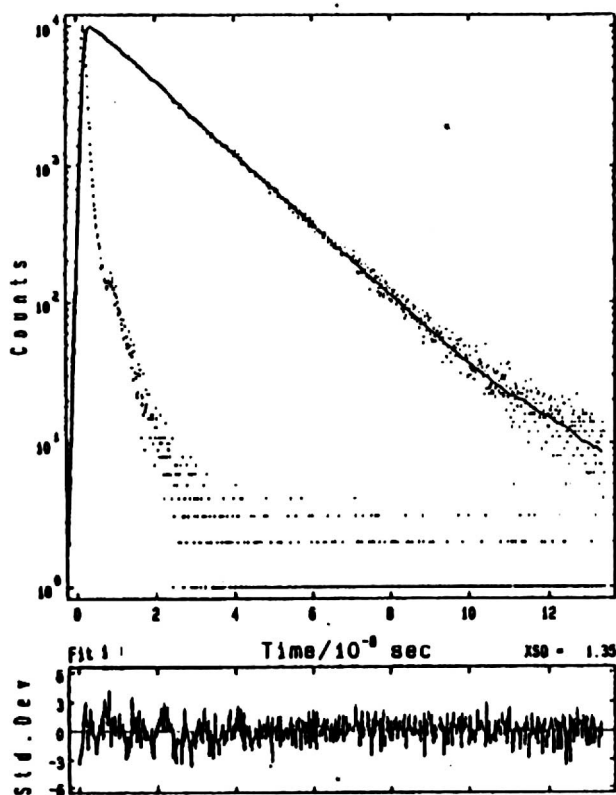


Fig. 5. Fluorescence decay profile of **2a** in acetonitrile in the presence of 7.4×10^{-4} M of $\text{Fe}(\text{H}_2\text{O})_6(\text{ClO}_4)_2$. Shown also in the figure is the excitation lamp profile. The excitation wavelength was 400 nm and the fluorescence was monitored at the emission band maximum. Solid-line indicates the best fit to the measured decay profile. The decay curve could be fitted to a single exponential decay function ($\tau = 16.8$ ns).

force (ΔG^*) for the PIET process is estimated to be feasible for all the systems, the actual extent of PIET in a fluorophore–spacer–receptor system also depends on the relative orientation and the effective distance between the fluorophore and receptor along with the medium of study. This may be true if we compare the f values (Table II), which are the direct experimental evidence for the PIET communication in the systems, and ΔG^* values shown in Table VI. Unlike their ΔG^* values, the f values for **1a**, **2a**, and **3a** are quite different as compared to those of **1b**, **2b**, and **3b**, respectively, and the latter series show enhanced PIET communication and hence much lowered fluorescence quantum yields (Table II).

The fluorescence decay behavior of the multicomponent systems further confirms the PIET process in the systems. As is shown in Fig. 3, the decay traces of the multicomponent systems could be best fitted to a biexponential fitting function. This indicates at least two species with different PIET interactions (a short-lived species with an

Table VI. Reduction Potentials and Singlet State Energies of **4**, **5**, and **6** and the Thermodynamic Driving Force (ΔG^*) for PIET Interaction in the Sensor Systems, **1**, **2**, and **3**

Fluorophore	E_{red} (fluor) (V) ^a	$E_{0,0}$ (kcal/mol) ^b	System	ΔG^* (kcal/mol) ^c
4	−1.61	55.04	1a	−6.6
			1b	−6.4
5	−1.66	62.2	2a	−12.7
			2b	−12.4
6	−1.11	65.3	3a	−28.4
			3b	−28.2

^aDetails of the measurement conditions are described in the experimental section; cyclic voltammetric traces for the reductions of **4** and **5** are irreversible and that of **6** is found to be reversible.

^b $E_{0,0}$ values have been estimated from the mean position of the absorption and emission band maxima of the fluorophores in acetonitrile.

^c E_{ox} values used in the ΔG^* calculation or adopted from Ref. [33]. The oxidation potentials of triethylamine and *N*-methylaniline were corrected for Ag/AgCl electrode by subtracting 0.27 V from the measured potentials against SCE electrode. The free energy change values are applicable in polar solvents such as acetonitrile.

efficient PIET interaction and a long-lived species having, presumably, inefficient or no PIET interaction between the components) exist in solution [34].⁸ The percentages of the short-lived components are, interestingly, high for **2** and **3** over **1**, and within one set of systems having the same fluorophore component, it is observed to be more for systems with the aniline moiety as the receptor (systems of series B). This clearly indicates order of efficiency of the PIET communication in these systems.

The changes in the fluorescence spectrum of **3b** in the presence of the metal ions are shown in Fig. 4, and FE values observed for various systems in the presence of the different metal ions in two solvents are presented in Tables IV and V. As it can be seen from the tables, the signaling efficiency of any system is directly related to the efficiency of the PIET interaction in the unbound state (ca. the f values depicted in Table II). Expected high FE values for systems **2** and **3**, having the electron deficient fluorophores **5** and **6**, respectively, in the presence of the transition metal ions is attributed for improved PIET interaction in the unbound state. Further improvements in the FE values for the systems of series B confirm the role of the PIET interaction in the development of efficient fluorosensors for the transition metal ions.

⁸The mechanism of the PIET process, effect of solvent and other factors on it have been clearly reported for many systems where the electron donor and the acceptor moieties (in the present case receptor and fluorophores moieties, respectively) are connected with a flexible aliphatic chains, as well as rigid spacer units between the reacting components.

To better understand the role of extent of the PIET interaction on the sensing efficiency of these systems, we have systematically explored the various interactions operative in the multicomponent systems in the absence and in the presence of the metal ions. In the absence of the metal ions, as evidenced by their low fluorescence quantum yields, the PIET interaction between the components is operating quite efficiently, especially in the systems with electron deficient fluorophores. On the other hand in the presence of the metal ions, the interaction between the fluorophore and the metal ion leads to fluorescence quenching and that between the receptor and the metal ion results in the FE. Therefore, the net result of these two opposite interactions (quenching or FE) is determined by the extents of quenching due to the former interaction and the enhancement due to the latter. However, as we addressed earlier, the quenching influence of the transition metal ions becomes unimportant when a strong PIET communication is operating in the system [8,9]. This can be elaborated as follows. Generally, the quenching efficiency of the metal ions could be obtained experimentally by using the Stern-Volmer equation [23], $I_0/I = 1 + k_q \tau_0 [Q]$, where I_0 is the initial fluorescence intensity, I is the intensity of the metal ion quenched fluorescence, k_q is the quenching constant, τ_0 is the fluorescence lifetime of the unquenched fluorophore and $[Q]$ represents the concentration of the quencher (transition metal ions in the present case). Assuming the same experimental conditions and the same metal ion used, the quenching efficiency of a specific metal ion on a system with strong PIET interaction is reduced by a factor that is equal to the ratio between the lifetimes of the nonquenched parent fluorophore and the PIET quenched multicomponent system. For example, if we consider fluorophore **6** and its multicomponent system **3** with lifetimes of 8.1 and 0.4 ns in acetonitrile, respectively, the quenching interaction of a metal ion towards **3** will reduce by a factor of ~ 20 . Or from the above equation, a 1 mM solution of the metal ion with a k_q value of $2.0 \times 10^{10} \text{ M}^{-1} \text{ s}^{-1}$ quenches the fluorescence intensity of **6** (using a lifetime of 8.1 ns in acetonitrile) by 14%, whereas the reduction in the fluorescence intensity of **3** (with a lifetime of 0.4 ns) is predicted to be insignificant (about 0.8%). The same reasoning can explain the differences in the quenching efficiencies of the metal ions on **1a** and **1b** and in other respective systems. When the PIET interaction in the multicomponent systems is efficient, the quenching influence of the transition metal ions becomes unimportant, and the FE is easily observed. Fine-tuning of the PIET interaction in the unbound state of the system will provide an excellent signaling device for any metal ion irrespective of its quenching efficiency.

CONCLUSIONS

Fluorescence spectral behavior of several structurally simple multicomponent systems has been studied in the absence and presence of transition metal ions. The high FE values observed for the systems having an efficient PIET interaction substantiate the role of PIET interaction in the metal sensing efficiency of a sensor system. The present study reveals that the fine-tuning of the PIET interaction between the fluorophore and receptor components for the development of an efficient sensor system is feasible by choosing an *electron deficient fluorophore* in the construction of the multicomponent sensor systems with *fluorophore–spacer–receptor* architecture. The systems with optimized PIET interaction can show excellent FE, irrespective of the quenching efficiency of the metal ions.

ACKNOWLEDGMENT

Author expresses his sincere gratitude to Professor Anunay Samanta of School of Chemistry, University of Hyderabad, Hyderabad, India for his helpful discussions.

REFERENCES

- (a) F. L. Carter, R. E. Siatkowski, and H. Wohltjen (Eds.) (1988). *Molecular Electronic Devices*; Elsevier, Amsterdam. (b) J. M. Lehn (1995). *Supramolecular Chemistry*; VCH, Weinheim. (c) V. Balzani, A. Juris, A. M. Venturi, S. Campagna, and S. Seroni (1996). Luminescent and redox-active polynuclear transition metal complexes. *Chem. Rev.* **96**(2), 759–833.
- (a) J. P. Desvergne and A. W. Czarnik (Eds.) (1997). *Chemosensors of Ion and Molecular Recognition*; NATO ASI Series C492, Kluwer Academic, Dordrecht. (b) A. P. de Silva, H. Q. N. Gunaratne, T. Gunnlaugsson, A. J. M. Huxley, C. P. McCoy, J. T. Rademacher, and T. E. Rice (1997). Signaling recognition events with fluorescent sensors and switches. *Chem. Rev.* **97**(5), 1515–1566. (c) B. Valeur (1994). In J. R. Lakowicz (Ed.). *Topics in Fluorescence Spectroscopy*, Vol. 4, Plenum Press, New York, p. 21. (d) T. D. James, P. Linnane, and S. Shinkai (1996). Fluorescent saccharide receptors: A sweet solution to the design, assembly and evaluation of boronic acid derived PET sensors. *Chem. Commun.* 281–288. (e) L. Fabbrizzi, M. Licchelli, P. Pallavicini, and D. Sacchi (1994). An anthracene-based fluorescent sensor for transition metal ions. *Angew. Chem. Int. Ed. Engl.* **33**(19), 1975–1977. (f) L. Prodi, F. Bolletta, M. Montalti, and N. Zaccheroni (2000). Luminescent chemosensors for transition metal ions. *Coord. Chem. Rev.* **205**, 59–83.
- (a) A. W. Czarnik (1994). Chemical communication in water using fluorescent chemosensors. *Acc. Chem. Res.* **27**(10), 302–308. (b) L. Fabbrizzi, M. Licchelli, P. Pallavicini, A. Perotti, A. Taglietti, and D. Sacchi (1996). Fluorescent sensors for transition metals based on electron-transfer and energy-transfer mechanisms, *Chem. Eur. J.* **2**(1), 75–82.
- (a) P. Ghosh, P. K. Bharadwaj, S. Mandal, and S. Ghosh (1996). Ni(II), Cu(II), and Zn(II) cryptate-enhanced fluorescence of a trianthrylcryptand: A potential molecular photonic OR operator. *J. Am. Chem. Soc.* **118**, 1553. (b) S. Banthia and A. Samanta (2002). Photophysical and transition metal ion signaling behavior of a three-component system comprising a cryptand moiety as the receptor. *J. Phys. Chem. A* **106**, 5572.

5. A. W. Varnes, R. B. Dodson, and E. L. Wehry (1972). Interactions of transition-metal ions with photoexcited states of flavines. Fluorescence quenching studies. *J. Am. Chem. Soc.* **94**(3), 946–950.
6. J. A. Kemlo and T. M. Shepherd (1977). Quenching of excited singlet states by metal ions. *Chem. Phys. Lett.* **47**(1), 158–162.
7. Ramachandram and A. Samanta (1997). Modulation of metal-fluorophore communication to develop structurally simple fluorescent sensors for transition metal ions. *Chem. Commun.* (11), 1037–1038.
8. B. Ramachandram and A. Samanta (1998). How important is the quenching influence of the transition metal ions in the design of fluorescent PET sensors? *Chem. Phys. Lett.* **290**(1–3), 9–16.
9. B. Ramachandram and A. Samanta (1998). Transition metal ion induced fluorescence enhancement of 4-(*N,N*-dimethylethylenediamino)-7-nitrobenz-2-oxa-1,3-diazole. *J. Phys. Chem. A* **102**, 10579–10587.
10. B. Ramachandram, N. B. Sankaran, and A. Samanta (1999). Fluorescence response of structurally simple fluorophore–spacer–receptor systems towards transition metal ions and protons. *Res. Chem. Intermed.* **25**(9), 843–859.
11. B. Ramachandram, N. B. Sankaran, R. Karmakar, S. Saha, and A. Samanta (2000). Fluorescence signaling of transition metal ions by multi-component systems comprising 4-chloro-1,8-naphthalimide as fluorophore. *Tetrahedron* **56**(36), 7041–7044.
12. B. Ramachandram, G. Saroja, N. B. Sankaran, and A. Samanta (2000). Unusually high fluorescence enhancement of some 1,8-naphthalimide derivatives induced by transition metal salts. *J. Phys. Chem. B* **104**, 11824.
13. R. Badugu (2002). Development of efficient fluorosensors for the transition metal ions by tuning of photoinduced intramolecular electron transfer (PIET) communication between the components. *Chem. Lett.* **52**.
14. D. D. Perrin, W. L. Armarego, and D. R. Perrin (1980). *Purification of Laboratory Chemicals*, Pergamon Press, New York.
15. C. Reichardt (1998) *Solvents and Solvent Effects in Organic Chemistry*; VCH, Weinheim, Chapter 7.
16. D. V. O'Connor and D. Phillips (1984). *Time-Correlated Single Photon Counting*; Academic Press, London.
17. K. Rechthaler and G. Köhler (1994). Excited state properties and deactivation pathways of 7-aminocoumarins. *Chem. Phys.* **189**(1), 99–116.
18. T. Soujanya, R. W. Fessenden, and A. Samanta (1996). Role of nonfluorescent twisted intramolecular charge transfer state on the photophysical behavior of aminophthalimide dyes. *J. Phys. Chem.* **100**(9), 3507–3512.
19. See for example, A. Zweig, A. H. Maurer, and B. G. Roberts (1967). Oxidation, reduction, and electrochemiluminescence of donor-substituted polycyclic aromatic hydrocarbons. *J. Org. Chem.* **32**(5), 1322–1329 and references cited therein.
20. Y. Q. Gao and R. A. Marcus (2002). Theoretical investigation of the directional electron transfer in 4-aminonaphthalimide compounds. *J. Phys. Chem. A* **106**(10), 1956–1960.
21. G. Saroja and A. Samanta (1994). Steady state and time-resolved studies on the redox behavior of 1,8-naphthalimide in the excited state. *J. Photochem. Photobiol. A Chem.* **84**(1), 19–26.
22. (a) D. Yuan and R. G. Brown (1997). Enhanced nonradiative decay in aqueous solutions of aminonaphthalimide derivatives via water-cluster formation. *J. Phys. Chem. A* **101**(19), 3461–3466. (b) M. S. Alexiou, V. Tychoopoulos, S. Ghorbanian, J. H. P. Tyman, R. G. Brown, and P. I. Brittain (1990). The UV–Visible absorption and fluorescence of some substituted 1,8-naphthalimides and naphthalic anhydrides. *J. Chem. Soc. Perkin Trans.* **2**(5), 837–842.
23. J. R. Lakowicz (1999). *Principles of Fluorescence Spectroscopy*, 2nd ed., Kluwer Academic/Plenum Publishers, New York.
24. (a) A. Pardo, E. Martin, J. M. L. Poyato, J. J. Camacho, M. F. Brana, and J. M. Castellano (1987). Synthesis and photophysical properties of some *N*-substituted-1,8-naphthalimides. *J. Photochem. Photobiol. A Chem.* **41**(1), 69–78. (b) A. Pardo, E. Martin, J. M. L. Poyato, J. J. Camacho, J. M. Guerra, R. Weigand, M. F. Brana, and J. M. Castellano (1989). *N*-substituted 1,8-naphthalimide derivatives as high efficiency laser dyes. *J. Photochem. Photobiol. A Chem.* **48**(2–3), 259–263. (c) A. Pardo, J. M. L. Poyato, E. Martin, J. J. Camacho, and D. Rayman (1990). Double exponential fluorescence decay in the protonation equilibrium of 4-methoxy-*N*-[2-(1-pyrrolidin)ethyl]-1,8-naphthalimide. *J. Lumin.* **46**(6), 381–385. (d) A. P. de Silva, H. Q. N. Gunaratne, T. Gunnlaugsson, and P. L. M. Lynch (1996). Molecular photoionic switches with an internal reference channel for fluorescent pH sensing applications. *New J. Chem.* **20**(7–8), 871–880.
25. (a) D. Noukakis, and P. Suppan (1991). Photophysics of aminophthalimides in solution. I. Steady-state spectroscopy. *J. Lumin.* **47**(6), 285–295. (b) E. Laitinen, K. Salonen, and T. O. Harju (1996). Solvation dynamics study of 4-amino-*N*-methyl-phthalimide in *n*-alcohol solutions. *J. Chem. Phys.* **104**(16), 6138–6148. (c) T. O. Harju, A. H. Huizer, and C. A. G. O. Varma (1995). Nonexponential salvation dynamics of electronically excited 4-aminophthalimide in *n*-alcohols. *Chem. Phys.* **200**, 215. (d) S. Das, A. Datta, and K. Bhattacharyya (1997). Deuterium isotope effect on 4-aminophthalimide in neat water and reverse micelles. *J. Phys. Chem. A* **101**(18), 3299–3304. (e) H. Langhals (1991). A simple, quick, and precise procedure for the determination of water in organic-solvents. *Anal. Lett.* **23**(12), 2243–2258.
26. T. Okada, T. Saito, T. Mataga, Y. Sakata, and S. Misumi (1977). *Bull. Chem. Soc. Jpn.* **50**, 331 and references cited therein.
27. J. W. Verhoeven, T. Schere, and R. J. Willems (1993). Solvent effects on the structure of fluorescent exciplexes in rigidly-bridged, flexibly-bridged, and non-bridged donor-acceptor systems. *Pure Appl. Chem.* **65**(8), 1717–1722.
28. (a) R. W. Kaplan, A. M. Napper, D. H. Waldeck, and M. B. Zimmt (2000). Solvent mediated coupling across 1 nm: Not a π -bond in sight. *J. Am. Chem. Soc.* **122**(48), 12039–12040. (b) H. Han and M. B. Zimmt (1998). Solvent-mediated electron transfer: Correlation between coupling magnitude and solvent vertical electron affinity. *J. Am. Chem. Soc.* **120**(31), 8001–8002.
29. R. S. Drago (1977). *Physical Methods in Chemistry*, Saunders College Publishing, Philadelphia.
30. (a) M. M. Martin, P. Plaza, N. Dai Hung, Y. H. Meyer, J. Bourson, and B. Valeur (1993). Photoejection of cations from complexes with a crown-ether-linked merocyanine evidenced by ultrafast spectroscopy. *Chem. Phys. Lett.* **202**(5), 425–430. (b) M. M. Martin, P. Plaza, Y. H. Meyer, L. Begin, J. Bourson, and B. Valeur (1994). A new concept of photogeneration of cations: Evidence for photoejection of Ca^{2+} and Li^{+} from complexes with a crown-ether-linked merocyanine by picosecond spectroscopy. *J. Fluorescence* **4**(4), 271–275. (c) M. M. Martin, P. Plaza, Y. H. Meyer, F. Badaoui, J. Bourson, J. P. Lefebvre, and B. Valeur (1996). Steady-state and picosecond spectroscopy of Li^{+} or Ca^{2+} complexes with a crowned merocyanine. Reversible photorelease of cations. *J. Phys. Chem.* **100**(17), 6879–6888. (d) B. Valeur and I. Leray (2000). Design principles of fluorescent molecular sensors for cation recognition. *Coord. Chem. Rev.* **205**, 3–40.
31. (a) J. -F. Letard, R. Lapouyade, and W. Rettig (1993). Synthesis and photophysical study of 4-(*N*-monoaza-15-crown-5)stilbenes forming TICT states and their complexation with cations. *Pure Appl. Chem.* **65**(8), 1705–1712. (b) P. Duman, G. Jonasauskas, F. Dupuy, P. Pee, C. Rulliere, J. -F. Letard, and R. Lapouyade (1994). Picosecond dynamics of cation-macrocycle interactions in the excited state of an intrinsic fluorescence probe: The calcium complex of 4-(*N*-monoaza-15-crown-5)-4'-phenylstilbene. *J. Phys. Chem.* **98**(41), 10391–10396. (c) R. Mathevet, G. Jonasauskas, C. Rulliere, J.-F. Letard, and R. Lapouyade (1995). Picosecond transient absorption as monitor of the stepwise cation-macrocycle decoordination in the excited singlet state of 4-(*N*-monoaza-15-crown-5)-4'-cyanostilbene. *J. Phys. Chem.* **99**(43), 15709–15713.
32. (a) A. Weller (1968). *Pure Appl. Chem.* **16**, 118. (b) D. Rehm and A. Weller (1970). *Isr. J. Chem.* **8**, 259.
33. H. Siegeman (1975). In N. L. Weinberg (Ed.), *Techniques of Chemistry*, Wiley, New York, Vol. V, Part II, p. 803.

34. See for example; (a) M. A. Fox and M. Chanon, (Eds.) (1998). *Photoinduced Electron Transfer*, Elsevier, New York, Parts A–D. (b) A. Weller, H. Staerk, and R. Trichel (1984). *Faraday Discuss. Chem. Soc.* **79**, 271. (c) D. Gust and T. A. Moore (1991). In *Photoinduced Electron Transfer* J. Mathey, (Ed.), *Topics in Current Chemistry* **159**, Vol. 3, Springer-Verlag, New York, p. 105. (d) J. W. Verhoeven (1990). Electron transport via saturated hydrocarbon bridges-exciplex emission from flexible rigid and semiflexible bichromophores. *Pure Appl. Chem.* **62**, 1585. (e) K. D. Jordan and M. N. Paddon-Row (1992). Analysis of the interactions responsible for long-range through-bond-mediated electronic coupling between remote chromophores attached to rigid polynorbornyl bridges. *Chem. Rev.* **92**(3), 395–410. (f) M. R. Wasielewski (1992). Photoinduced electron transfer in supramolecular systems for artificial photosynthesis. *Chem. Rev.* **92**(3), 435–461. (g) G. J. Kavarnos (1993) *Fundamentals of Photoinduced Electron Transfer*, VCH, New York. (h) S. Speiser (1996). Photophysics and mechanisms of intramolecular electronic Energy transfer in bichromophoric molecular systems: Solution and supersonic jet studies. *Chem. Rev.* **96**(6), 1953–1976. (i) J. M. Warman, S. A. Jonker, W. Schuddeboom, M. P. de Haas, M. N. Paddon-Row, J. W. Verhoeven, and K. A. Zachariasse (1993). Straight, bent and twisted intramolecular charge separated states as seen by time-resolved microwave conductivity (TRMC). *Pure Appl. Chem.* **65**(8), 1723–1728. (j) A. Napper, I. Read, D. H. Waldeck, N. J. Head, A. M. Oliver, and M. N. Paddon-Row (2000). An unequivocal demonstration of the importance of nonbonded contacts in the electronic coupling between electron donor and acceptor units of donor-bridge-acceptor molecules. *J. Am. Chem. Soc.* **122**(21), 5220–5221. (k) I. Read, A. Napper, M. B. Zimmt, and D. H. Waldeck (2000). Electron transfer in aromatic solvents: The importance of quadrupolar interactions. *J. Phys. Chem. A* **104**(41), 9385–9394. (l) I. Read, A. Napper, R. Kaplan, M. B. Zimmt, and D. H. Waldeck (1999). Solvent-mediated electronic coupling: The role of solvent placement. *J. Am. Chem. Soc.* **121**(47), 10976–10986. (m) R. J. Cave, M. D. Newton, K. Kumar, and M. B. Zimmt (1995). Theoretical study of solvent effects on the electronic coupling matrix element in rigidly linked donor-acceptor systems. *J. Phys. Chem.* **99**(49), 17501–17504.